haematologica
Journal of the Ferrata Storti Foundation

Morphologic and immunophenotypic characterization of lymphocytosis following BCMA-targeted CAR-T cell therapy in relapsed/refractory multiple myeloma

by Jiani N. Chai, Paul Dennis Simonson, Kameisha Gulgar, Frank Costanzo, David S. Jayabalan, Mark Bustoros, Giorgio Ga. Inghirami, Julia T. Geyer and Mateo Mejia Saldarriaga

Received: September 2, 2025.
Accepted: January 16, 2026.

Citation: Jiani N. Chai, Paul Dennis Simonson, Kameisha Gulgar, Frank Costanzo, David S. Jayabalan, Mark Bustoros, Giorgio Ga. Inghirami, Julia T. Geyer and Mateo Mejia Saldarriaga. Morphologic and immunophenotypic characterization of lymphocytosis following BCMA-targeted CAR-T cell therapy in relapsed/refractory multiple myeloma.
Haematologica. 2026 Jan 29. doi: 10.3324/haematol.2025.289079 [Epub ahead of print]

Morphologic and immunophenotypic characterization of lymphocytosis following BCMA-targeted CAR-T cell therapy in relapsed/refractory multiple myeloma

Jiani N. Chai[1], Paul Dennis Simonson[1], Kameisha Gulgar[1], Frank Costanzo[1], David S. Jayabalan[2], Mark Bustoros[2], Giorgio Ga. Inghirami[1], Julia T. Geyer[1$], Mateo Mejia Saldarriaga[2$]

$These authors contributed equally as senior authors

[1] Department of Pathology and Laboratory Medicine, Weill Cornell Medicine, New York, NY, USA

[2] Division of Hematology & Medical Oncology, Meyer Cancer Center, Weill Cornell Medicine, New York, NY, USA

Corresponding author:

Mateo Mejia Saldarriaga, MD

Email: mam9823@med.cornell.edu

Julia T. Geyer, MD

Email: jut9021@med.cornell.edu

Running head:

Immunophenotype of Lymphocytosis After BCMA CAR-T

Authors' contributions:
JNC contributed to the review of peripheral blood smears, data analysis, and manuscript drafting. PDS contributed to flow cytometric data analysis and manuscript review. KG and FC contributed to flow cytometric sample processing, data acquisition, and data analysis. DSJ contributed to the collection of clinical patient data and samples. MB contributed to study design, clinical patient data collection, and manuscript review.

GGI contributed to study design, data analysis, flow cytometric sample processing, and manuscript review. JTG contributed to study design, peripheral blood smear review, data analysis, and manuscript review. MMS contributed to study design, clinical patient data collection, data analysis, and manuscript review.

Disclosures:

MMS: Speaker Bureau for Johnson & Johnson. The other authors declare no conflict of interest.

Funding:

The authors received no specific funding for this work.

Acknowledgments:

We thank the immunopathology laboratory staff at Weill Cornell Medicine for their assistance with sample processing and data acquisition.

Data-sharing statement:

The datasets generated and analyzed in this study are available from the corresponding author on reasonable request.

B-cell maturation antigen (BCMA)-targeting chimeric antigen receptor T cell (CAR-T) therapy has emerged as a standard treatment for relapsed/refractory multiple myeloma (R/R MM)[1]. The U.S. Food and Drug Administration has approved two autologous BCMA-targeted CAR-T cell products: ciltacabtagene autoleucel (cilta-cel) and idecabtagene vicleucel (ide-cel). These approvals were based on robust clinical trial data showing overall response rates exceeding 70% in heavily pretreated patients[2,3].

A well-established phenomenon following CAR-T therapy is the in vivo expansion of infused T cells, which correlates with both therapeutic efficacy and immune-related toxicities such as cytokine release syndrome (CRS)[4–6]. Transient post-infusion lymphocytosis has been observed in R/R MM following BCMA CAR-T infusion. In this context, the absolute lymphocyte count (ALC) serves as a surrogate marker for CAR-T expansion, typically peaking around Days +11 to +12. Higher maximum ALC (ALC_{max}) has been associated with improved depth of response, longer progression-free survival, and more durable remissions[7–9].

The cytomorphology and immunophenotype of the expanded CAR-T cells in BCMA-directed therapies remain poorly characterized, posing diagnostic challenges in the post-infusion period. Additionally, BCMA CAR-T therapy is associated with neurotoxicities beyond CRS. These include immune effector cell-associated neurotoxicity syndrome (ICANS) and a distinct delayed non-ICANS neurotoxicity, the latter of which is not typically observed in CD19 CAR-T therapy. A recent study demonstrated that higher ALC_{max} correlates with the timing of CRS and ICANS onset[9]. However, the relationship between CAR-T expansion kinetics, subset composition, and these toxicities remains unclear.

Here, we present a combined retrospective and prospective analysis aimed at characterizing the morphologic and immunophenotypic features of lymphocytosis following BCMA CAR-T infusion in R/R MM patients. To our knowledge, this is the first study utilizing standard-of-care flow cytometry to measure BCMA CAR-T kinetics in the peripheral blood (PB) following infusion. We specifically addressed the diagnostic challenges encountered during routine clinical follow-up, including the morphologic features of expanded CAR-T cells and their immunophenotypic profiles. Additionally, we monitored the longitudinal dynamics of CAR-T cells, including ALC and CAR-T expansion kinetics and subset composition, providing further insight into the cellular dynamics underlying therapeutic response and their potential association with neurotoxicity. The Institutional Review Board of Weill Cornell Medicine approved this study.

We initially conducted a retrospective analysis of six patients with R/R MM who received BCMA CAR-T therapy between 2023 and 2024 and underwent PB flow cytometry due to marked post-infusion lymphocytosis. A total of seven PB specimens from these

patients were included. Patient characteristics, lymphocyte counts, and flow cytometric immunophenotyping data were collected and summarized (Supplementary Table 1). Corresponding PB smear slides were reviewed by board-certified hematopathologists to characterize the morphology of the lymphocytes. Flow cytometry used standard T cell markers and fluorophore-conjugated BCMA protein to detect CAR-T cells specifically.

All of the seven post-infusion specimens (Days 10–28) demonstrated elevated lymphocyte counts (range: 1.7–26 $\times 10^9$/L; median 2.7 $\times 10^9$/L). Atypical lymphocytes constituted 6%–82% (median: 53%) of total lymphocytes. Morphologically, smears revealed large, atypical lymphocytes with abundant pale blue cytoplasm and occasional cytoplasmic granules (Figure 1A).

Flow cytometry showed a predominance of CD3+ T cells (range: 16–99%; median: 98%), with frequent partial loss of CD7 (range: 10.2%–54.4%; median: 24.1%) and CD5 (range: 7%–17.2%; median: 9.2%) (Figure 1B). These aberrant populations included both CD4+ and CD8+ T cells, though CD8+ cells were more frequently predominant. All samples exhibited a decreased CD4:CD8 ratio. In one patient (Day +10), CD45 downregulation resulted in a significant proportion of T cells being classified within the “blast” gate in the CD45 versus side scatter plot (33.6%, Figure 1C). Fluorophore-conjugated BCMA protein confirmed the presence of expanded BCMA CAR-T cells in all tested patients (n=4, Figure 1D).

Following this observation, we collected samples from twenty-one R/R MM patients receiving BCMA CAR-T therapy for longitudinal monitoring of CAR-T kinetics through flow cytometry. Patient characteristics for this cohort are summarized (Supplementary Table 2). PB samples were collected at intervals from Day 0 to Week 30. ALC and BCMA CAR-T cell frequencies among total CD3+ T cells were quantified (Supplementary Table 3).

Consistent with our previous report[7], ALC_{max} was observed around two weeks post-infusion (Days +11 to +12) (Figure 2A). Flow cytometry demonstrated a parallel expansion of BCMA CAR-T cells during this period (Figure 2B). At the peak of expansion, CAR-T cells accounted for 6.6% to 86.5% of the CD3+ T cells in individual patients, with a median of 56.6%. By week six, CAR-T cells were undetectable in most patients, though three patients exhibited persistent CAR-T cells through weeks seven to nine.

Although a predominance of CD8+ BCMA CAR-T cell expansion was reported in a prior cohort[10], in our study, the proportion of CD4+ or CD8+ CAR-T cells varied among individual patients. Specifically, 10 of 21 patients (47.6%) demonstrated predominant $CD4^+$ CAR-T expansion, whereas 11 of 21 patients (52.4%) had a predominance of $CD8^+$ CAR-T cells (Figures 2C-D). This inter-individual variability in CD4/CD8 predominance within the CAR-T cell populations suggests heterogeneity in the

composition of the infusion products or differences in in vivo expansion dynamics. As reported for CD19 CAR-T cells, the CD4+/CD8+ ratio varied among the infusion products[11].

CRS and neurotoxicities, including ICANS and delayed neurotoxicity, are significant toxicities linked to BCMA CAR-T cell therapy. While CRS and ICANS are driven by cytokine release following the activation of CAR T cells, delayed neurotoxicity is thought to result from CAR-T cell infiltration into the central nervous system. In our prospective cohort, the majority of patients (19/21, 90.5%) developed CRS of varying severity. ICANS was observed in 4 of 21 patients (19.0%), and delayed neurotoxicity occurred in a similar proportion (4/21, 19.0%). Patients who developed ICANS or delayed neurotoxicity generally had higher ALC_{max} values compared with those without neurotoxicity. Among patients with $ALC_{max} \geq 3 \times 10^9/L$[12], 25.0% (3/12) developed ICANS and 33.3% (4/12) developed delayed neurotoxicity, compared to 11.1% (1/9) and 0% in those with $ALC_{max} < 3 \times 10^9/L$. Neurotoxicity was also strongly associated with the degree of CAR-T expansion. Patients with ≥60% BCMA+ CAR-T cells among total T cells showed higher rates of neurotoxicity. In this group, 44.4% (4/9) developed ICANS and 44.4% (4/9) developed delayed neurotoxicity. In contrast, no cases of either type of toxicity were observed in patients with <60% BCMA+ CAR-T cells (Fisher's exact test, *P* = 0.0211 for both comparisons) (Figures 2E-F; Supplementary Tables 2-3). In addition, ICANS was more frequent in patients with predominant CD4+ CAR-T expansion (3/10, 30%) than in those with predominant CD8+ expansion (1/11, 9.1%). Likewise, delayed neurotoxicity was more common in the CD4+ predominant group (3/10, 30%) compared with the CD8+ predominant group (1/11, 9.1%) (Figures 2G-H; Supplementary Tables 2-3). Flow cytometric analysis of the cerebrospinal fluid (CSF) was performed in one patient with delayed neurotoxicity, revealing a substantial population of BCMA CAR-T cells, predominantly of the CD4+ phenotype (Figure 2I). Although limited by a small sample size, these findings suggest that both the expansion kinetics and the predominance of CD4+ CAR-T cells may contribute to neurotoxicity. In this limited cohort, the factors associated with higher risk include higher ALCmax ($\geq 3 \times 10^9/L$), greater proportion of BCMA+ CAR-T cells (≥60% of total T cells), and CD4+ predominant CAR-T expansion. Larger cohort studies will be necessary to investigate this relationship further, and although BCMA CAR-T cells have been detected in the CSF of patients with delayed neurotoxicity[13], CSF data from patients without neurotoxicity are lacking, so it is unclear if traffic of CAR-T is routinely seen or truly associated with neurotoxicity.

Lastly, we examined T cell subset composition following CAR-T infusion. Previous studies in CD19-directed CAR-T therapies have shown that specific memory T cell phenotypes are associated with improved clinical responses[14,15]. T cell subset characterization included naive T cell (Tn; CD62L+CD45RA+CD45RO−), effector

memory T cell (Tem; CD62L−CD45RA−CD45RO+/−), and central memory T cell (Tcm; CD62L+CD45RA−CD45RO+) populations (Figure 3A). Similar to prior observations[10], we found a marked increase in CD4+ and CD8+ Tem and CD8+ Tcm subsets at the time of peak CAR-T expansion compared to baseline (collected on Day -5 or Day 0). Conversely, CD4+ and CD8+ naive T-cell subsets were significantly decreased at peak expansion relative to baseline (Figure 3B-I). The shift from naïve to memory phenotype suggests robust memory differentiation during CAR-T expansion.

In summary, our study provides a detailed morphologic and immunophenotypic analysis of lymphocytosis following BCMA-targeted CAR-T cell therapy in patients with R/R MM. We demonstrate that the post-infusion lymphocytosis observed in these patients is primarily driven by CAR-T cell expansion, which is accompanied by distinct morphologic features and immunophenotypic changes. The ALC_{max} and CAR-T expansion typically occurred approximately two weeks post-infusion, and both the magnitude and phenotype of expansion may contribute to neurotoxicity risk. Subset analysis reveals a preferential expansion of Tem and Tcm cells, alongside a reduction in Tn populations. The use of fluorophore-conjugated BCMA protein enables the reliable detection of CAR-T cells using conventional flow cytometry. These findings highlight the importance of integrating clinical context with flow cytometric and morphologic data to differentiate reactive lymphocytosis from disease progression or secondary lymphoproliferative disorders. The results have practical implications for the clinical interpretation of post-CAR-T lymphocytosis and for future studies that aim to explore the relationship between CAR-T expansion dynamics, cell composition at apheresis/infusion, efficacy, and toxicity.

References

1. Raje N, Berdeja J, Lin Y, et al. Anti-BCMA CAR T-Cell Therapy bb2121 in Relapsed or Refractory Multiple Myeloma. N Engl J Med. 2019;380(18):1726-1737.
2. Munshi NC, Anderson LD, Shah N, et al. Idecabtagene Vicleucel in Relapsed and Refractory Multiple Myeloma. N Engl J Med. 2021;384(8):705-716.
3. Martin T, Usmani SZ, Berdeja JG, et al. Ciltacabtagene Autoleucel, an Anti-B-cell Maturation Antigen Chimeric Antigen Receptor T-Cell Therapy, for Relapsed/Refractory Multiple Myeloma: CARTITUDE-1 2-Year Follow-Up. J Clin Oncol. 2023;41(6):1265-1274.
4. Wittibschlager V, Bacher U, Seipel K, et al. CAR T-Cell Persistence Correlates with Improved Outcome in Patients with B-Cell Lymphoma. Int J Mol Sci. 2023;24(6):5688.
5. Wei J, Liu Y, Wang C, et al. The model of cytokine release syndrome in CAR T-cell treatment for B-cell non-Hodgkin lymphoma. Signal Transduction and Targeted Therapy. Signal Transduct Target Ther. 2020;5(1):134.
6. Faude S, Wei J, Muralidharan K, et al. Absolute lymphocyte count proliferation kinetics after CAR T-cell infusion impact response and relapse. Blood Adv. 2021;5(8):2128-2136.
7. Mejia Saldarriaga M, Pan D, Unkenholz C, et al. Absolute lymphocyte count after BCMA CAR-T therapy is a predictor of response and outcomes in relapsed multiple myeloma. Blood Adv. 2024;8(15):3859-3869.
8. Fischer L, Grieb N, Born P, et al. Cellular dynamics following CAR T cell therapy are associated with response and toxicity in relapsed/refractory myeloma. Leukemia. 2024;38(2):372-382.
9. Dingli S, Rothweiler P, Binder M, et al. Implications of lymphocyte kinetics after chimeric antigen receptor T cell therapy for multiple myeloma. Leukemia. 2025;39(4):1005-1008.
10. Fischer L, Grieb N, Born P, et al. Cellular dynamics following CAR T cell therapy are associated with response and toxicity in relapsed/refractory myeloma. Leukemia. 2024;38(2):372-382.
11. Galli E, Bellesi S, Pansini I, et al. The CD4/CD8 ratio of infused CD19-CAR-T is a prognostic factor for efficacy and toxicity. Br J Haematol. 2023;203(4):564-570.

12. Lim KJC, Parrondo RD, Chhabra S, et al. Investigating the association between peak post-infusion absolute lymphocyte count (ALC) and delayed toxicity in myeloma (MM) patients (pts) receiving cilta-cel. J Clin Oncol. 2025;43(16_suppl):7522.

13. Kumar AD, Atallah-Yunes SA, Rajeeve S, et al. Delayed Neurotoxicity after CAR-T in Multiple Myeloma: Results from a Global IMWG Registry. Blood. 2024;144(Supplement 1):4758.

14. Turtle CJ, Hanafi L-A, Berger C, et al. CD19 CAR-T cells of defined CD4+:CD8+ composition in adult B cell ALL patients. J Clin Invest. 2016;126(6):2123-2138.

15. Haradhvala NJ, Leick MB, Maurer K, et al. Distinct cellular dynamics associated with response to CAR-T therapy for refractory B cell lymphoma. Nat Med. 2022;28(9):1848-1859.

Figure Legends

Figure 1. Morphologic and immunophenotypic features of lymphocytosis following BCMA CAR-T cell therapy.

(A) Atypical lymphocytes identified on peripheral blood smear following BCMA CAR-T cell infusion. (B) A representative flow cytometry plot demonstrating immunophenotypic features of T-lymphocytosis post BCMA CAR-T infusion (Day +11). (C) A flow cytometry plot showing marked downregulation of CD45 in T-cells from one patient (Day +10). (D) Detection of expanded CAR-T cells using fluorophore-labeled BCMA protein, confirming substantial in vivo proliferation (Day +10).

Figure 2. Kinetics of lymphocytosis, BCMA CAR-T cell expansion and association with neurotoxicity.

(A) The kinetics of the ALC post-infusion across twenty-one patients (data derived from complete blood counts). (B) The expansion kinetics of BCMA CAR-T cells post-infusion, as detected by flow cytometry using fluorophore-labeled BCMA protein. (C) Individual percentages of CD4+ and CD8+ CAR-T cells. (D) A cohort-level summary of CD4+/CD8+ CAR-T cell percentages. (E-H) Scatter plots showing relationships between CAR-T expansion parameters and neurotoxicity outcomes. Each point represents an individual patient (n=21). (E) Association of ALC_{max}/BCMA CAR-T percentage with ICANS. (F) Association of ALC_{max}/BCMA CAR-T percentage with delayed neurotoxicity. (G) Association of CD4+/CD8+ CAR-T percentage with ICANS. (H) Association of CD4+/CD8+ CAR-T percentage with delayed neurotoxicity. (I) Detection of expanded CAR T cells in the CSF of a patient with ICANS using fluorophore-conjugated BCMA protein.

Figure 3. Alterations in T-cell subset composition following BCMA CAR-T cell infusion.

(A) A representative flow cytometry plot illustrating the gating strategy for the delineation of T cell subsets: naive T-cells (Tn; CD62L+CD45RA+CD45RO−), effector memory T-cells (Tem; CD62L−CD45RA−CD45RO+/−), and central memory T-cells (Tcm; CD62L+CD45RA−CD45RO+). (B-G) Comparative analysis of T-cell subsets at baseline (Day −5 or 0) and at peak CAR-T expansion: (B) CD4+ naive T-cells. (C) CD4+ effector memory T-cells. (D) CD4+ central memory T-cells. (E) CD8+ naive T-cells. (F) CD8+ effector memory T-cells. (G) CD8+ central memory T-cells. (H-I) Summary plots showing the overall distribution of T-cell subsets at baseline and peak CAR-T expansion.

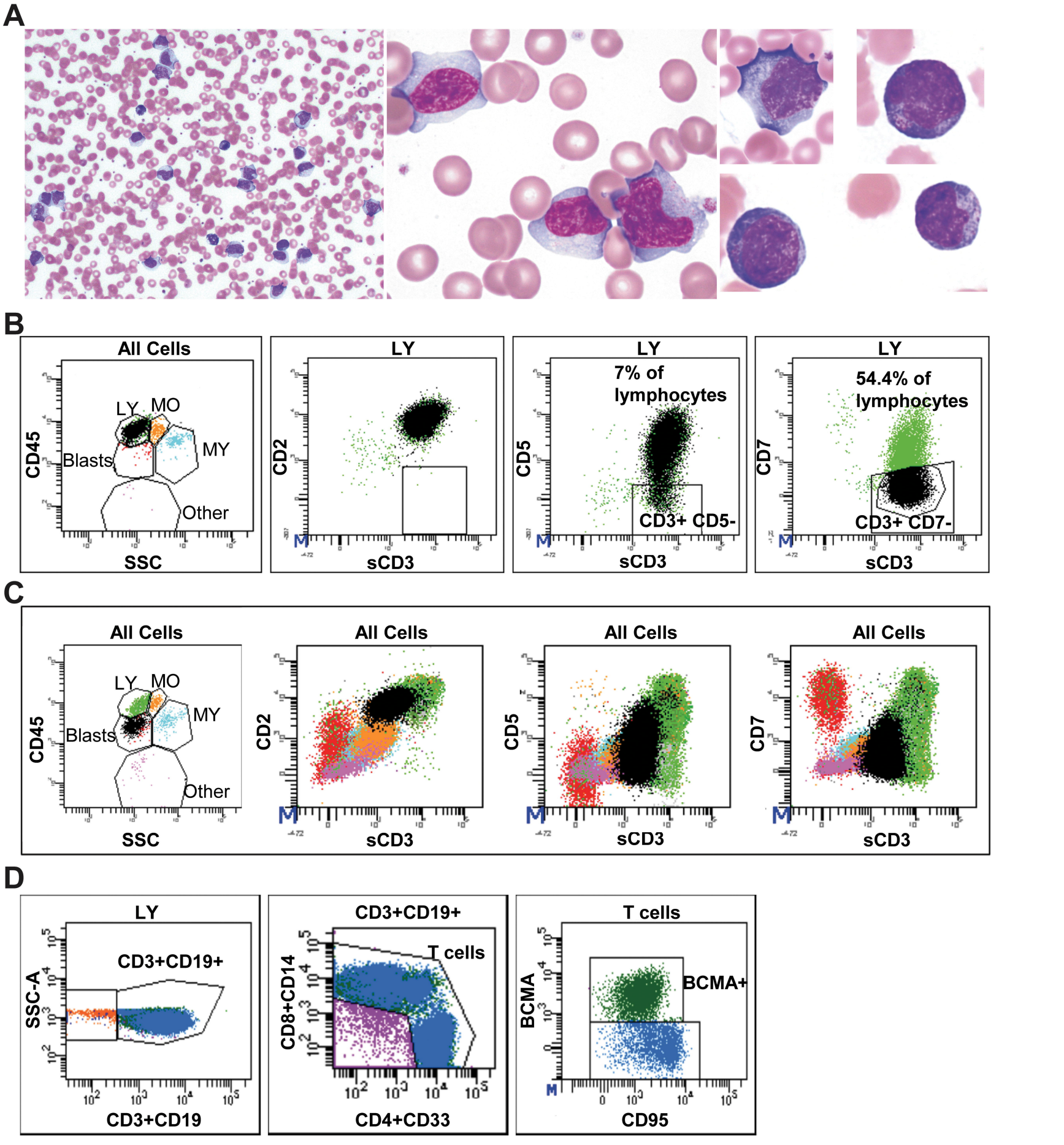
A
B
All Cells
LY
MO
MY
Blasts
Other
CD45
SSC
LY
CD2
sCD3
LY
7% of lymphocytes
CD5
CD3+ CD5-
sCD3
LY
54.4% of lymphocytes
CD7
CD3+ CD7-
sCD3
C
All Cells
LY
MO
MY
Blasts
Other
CD45
SSC
All Cells
CD2
sCD3
All Cells
CD5
sCD3
All Cells
CD7
sCD3
D
LY
CD3+CD19+
SSC-A
CD3+CD19
CD3+CD19+
T cells
CD8+CD14
CD4+CD33
T cells
BCMA+
BCMA
CD95

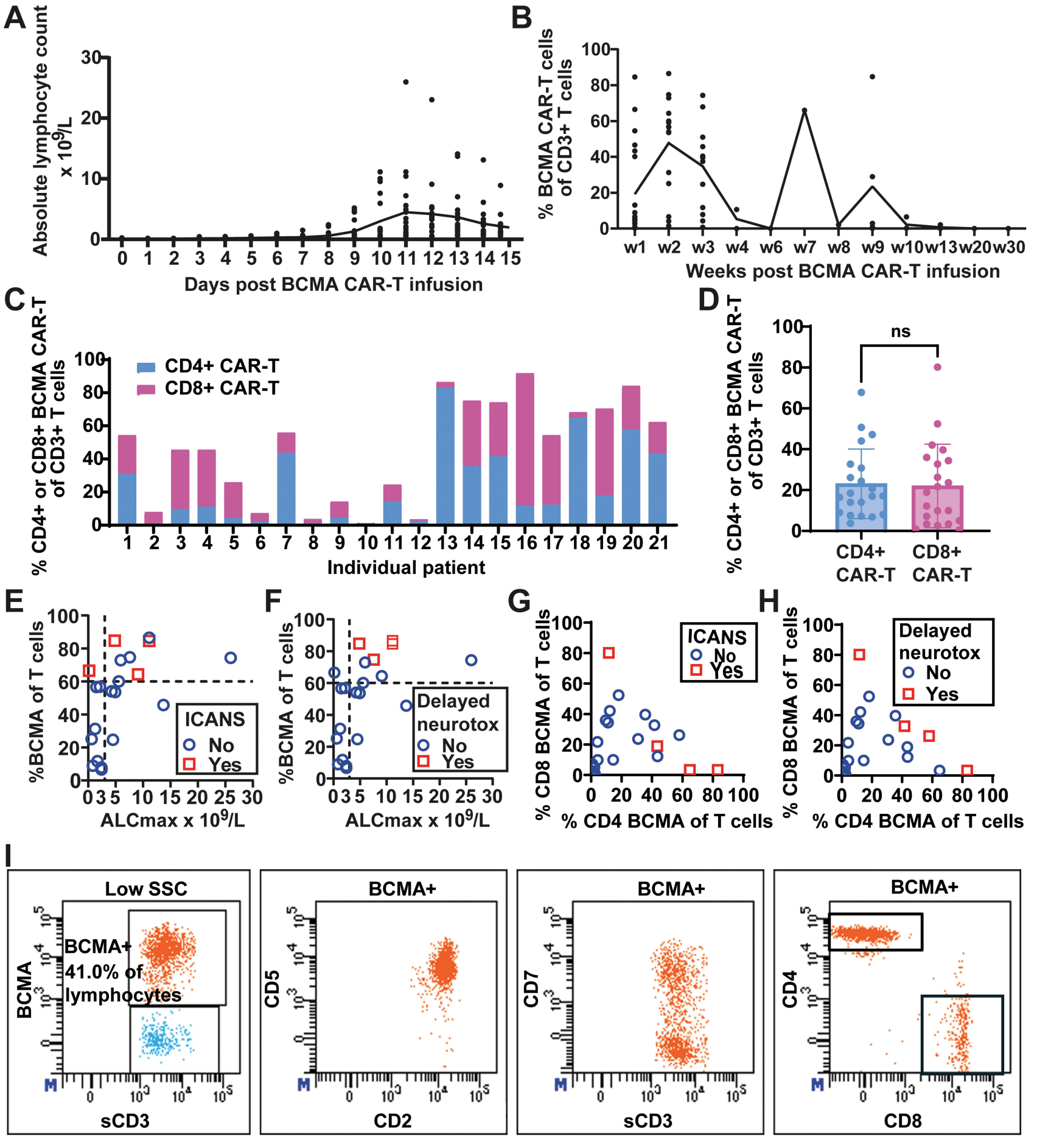
A
Absolute lymphocyte count x 10^9/L
Days post BCMA CAR-T infusion
B
% BCMA CAR-T cells of CD3+ T cells
w1 w2 w3 w4 w6 w7 w8 w9 w10 w13 w20 w30
Weeks post BCMA CAR-T infusion
C
% CD4+ or CD8+ BCMA CAR-T of CD3+ T cells
CD4+ CAR-T
CD8+ CAR-T
Individual patient
D
% CD4+ or CD8+ BCMA CAR-T of CD3+ T cells
ns
CD4+ CAR-T
CD8+ CAR-T
E
%BCMA of T cells
ICANS
No
Yes
ALCmax x 10^9/L
F
%BCMA of T cells
Delayed neurotox
No
Yes
ALCmax x 10^9/L
G
% CD8 BCMA of T cells
ICANS
No
Yes
% CD4 BCMA of T cells
H
% CD8 BCMA of T cells
Delayed neurotox
No
Yes
% CD4 BCMA of T cells
I
Low SSC
BCMA+
41.0% of lymphocytes
BCMA
sCD3
BCMA+
CD5
CD2
BCMA+
CD7
sCD3
BCMA+
CD4
CD8

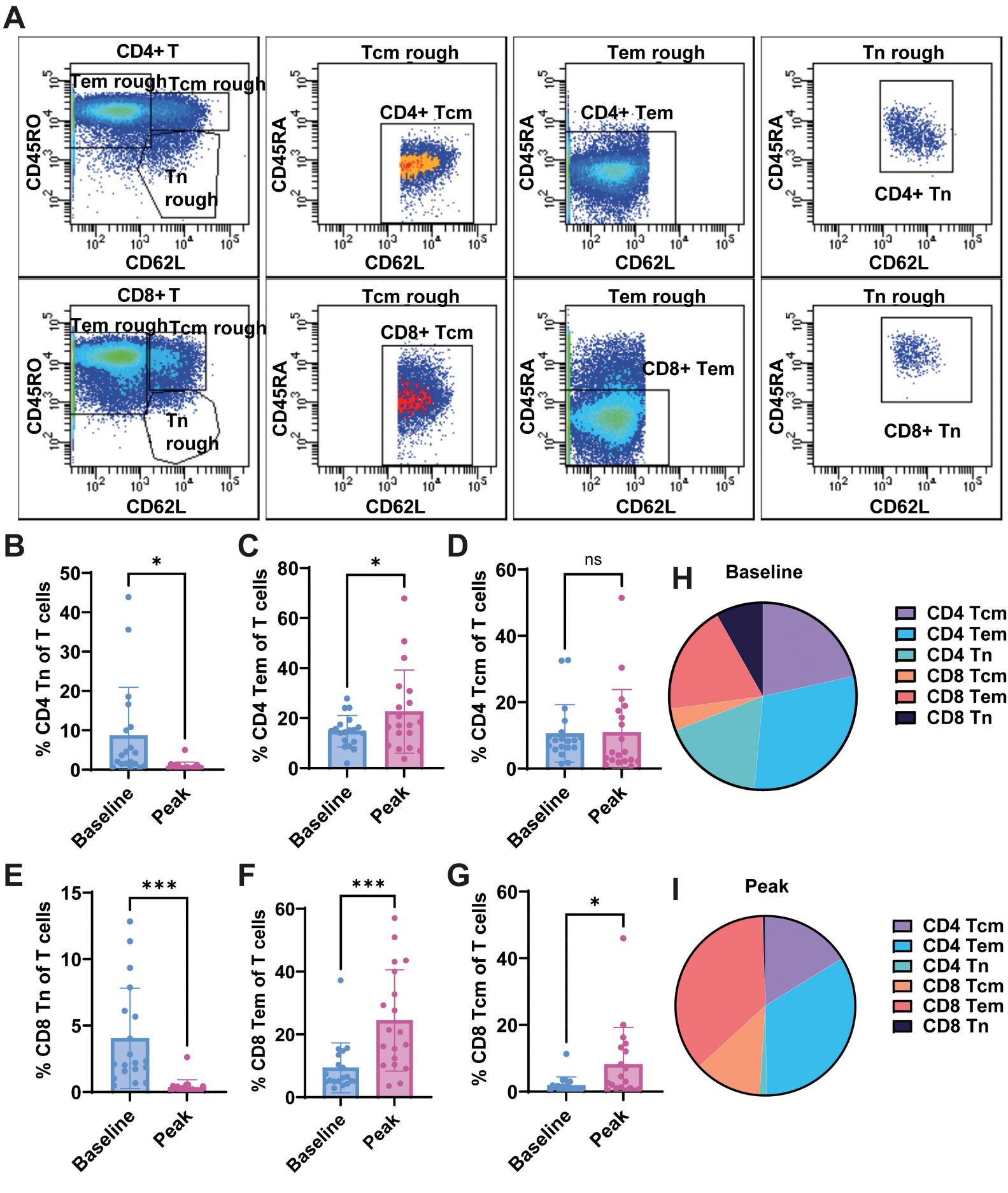
A
CD4+ T
Tem rough
Tcm rough
Tn rough
CD45RO
CD62L
CD8+ T
Tcm rough
Tem rough
Tn rough
CD45RA
CD62L
CD4+ Tcm
CD4+ Tem
CD4+ Tn
CD8+ Tcm
CD8+ Tem
CD8+ Tn
B
% CD4 Tn of T cells
C
% CD4 Tem of T cells
D
% CD4 Tcm of T cells
ns
E
% CD8 Tn of T cells
F
% CD8 Tem of T cells
G
% CD8 Tcm of T cells
Baseline
Peak
H
Baseline
I
Peak
CD4 Tcm
CD4 Tem
CD4 Tn
CD8 Tcm
CD8 Tem
CD8 Tn

Supplementary Table 1. Summary of patient characteristics, complete blood count (CBC), and flow cytometric findings post–BCMA CAR-T infusion in the retrospective cohort.

ID	Age	Gender	ISS stage	Days Post CAR-T	WBC $\times 10^9$/L	ALC $\times 10^9$/L	Atypical Lymphocytes (%)	Flow Cytometry Findings						
								% CD3+ of lymphocytes	% CD3+ CD7- of T cells	% CD3+ CD5- of T cells	CD4: CD8 ratio	% T cells in blast gate of total cells	Plasma Cells	%CAR-T of CD3 cells
1	56	M	II	D10	3.6	2.2	62	99	24.1	10.5	0.4	33.6	Absent	NA
				D14	3.0	1.7	57	97	17.7	11.2	0.5	7.4	Absent	59.9 (D14)
2	65	F	II	D11	32.5	26.0	82	99	54.4	7.0	0.73		Absent	59.2 (D10)
3	63	F	I	D11	4.0	2.7	53	98	10.2	9.2	0.2		Absent	NA
4	59	F	I	D13	15.4	13.7	52	99	44.4	8.4	1		Absent	56.9 (D14)
5	69	M	III	D14	7.1	5.6	45	94	23.2	17.2	0.1		Absent	NA
6	75	F	I	D28	6.1	1.7	6	16	29.8	4.0	0.8		Absent	60 (D14)

Note: All patients in this cohort received cilta-cel.

Supplementary Table 2. Baseline characteristics and association of expansion features with neurotoxicity in the prospective cohort (n = 21).

Top: Baseline demographic and clinical characteristics of patients receiving BCMA-directed CAR-T therapy.

Variable	All patients n=21
Gender, n (%)	
Female	9 (42.9)
Male	12 (57.1)
Age at diagnosis, median (range)	58 (42-72)
Year Car-T infusion, n (%)	
2023	9 (42.9)
2024	8 (38.1)
2025	4 (19.0)
CAR-T product, n (%)	
Cilta-cel	19 (90.5)
Ide-cel	2 (9.5)
ISS stage, n (%)	
Stage I	11 (52.4)
Stage II	4 (19.0)
Stage III	3 (14.3)
Unknown	3 (14.3)
Presence of cytokine release syndrome, n (%)	19 (90.5)
Grade I	10 (47.6)
Grade II	7 (33.3)
Grade III	2 (9.5)
Presence of immune effector cell-associated neurotoxicity syndrome	4 (19.0)
Presence of delayed neurotoxicity	4 (19.0)

Bottom: Association of CAR-T expansion features with neurotoxicity.

Group	Total (n)	ICANS, n (%)	Delayed neurotoxicity, n (%)
ALCmax ≥3 × 10^9/L	12	3 (25.0)	4 (33.3)
ALCmax <3 × 10^9/L	9	1 (11.1)	0 (0)
%BCMA of T cells ≥60%	9	4 (44.4)	4 (44.4)
%BCMA of T cells <60%	12	0 (0)	0 (0)
CD4-predominant CAR-T expansion	10	3 (30.0)	3 (30.0)
CD8-predominant CAR-T expansion	11	1 (9.1)	1 (9.1)

Supplementary Table 3. Summary of absolute lymphocyte count (ALC) kinetics, $BCMA^{+}$ CAR-T cell expansion, and associated toxicities in patients receiving BCMA-directed CAR-T therapy (n = 21).

ID	Gender	Age at diagnosis	Date CAR-T infusion	Car-T product	ISS stage	ALC_d minus5	ALC_d0	ALC_d1	ALC_d2	ALC_d3	ALC_d4	ALC_d5	ALC_d6	ALC_d7	ALC_d8
p1	Female	62	6/12/2023	Cilta-cel	II	1.83	0.02	0.03	0.04	0.04	0.06	0.12	0.3	0.33	0.36
p2	Female	72	7/17/2023	Cilta-cel	I	2	0.07	0.1	0.17	0.19	0.15	0.23	0.24	0.12	0.13
p3	Female	42	9/12/2023	Cilta-cel	I	0.4	0.01	0.09	0.06	0.1	0.19	0.13	0.13		
p4	Male	47	9/12/2023	Cilta-cel	II	1.1	0.07	0.03		0.15	0.19	0.39	0.33	0.08	0.34
p5	Male	61	9/11/2023	Cilta-cel	III	1.13	0.02	0.02	0.02	0.03	0.07	0.05	0.13	0.2	0.27
p6	Male	54	9/20/2023	Cilta-cel	III	0.88	0.04	0.07	0.14	0.16	0.26	0.26	0.42	0.5	0.37
p7	Female	67	11/6/2023	Cilta-cel	I	0.87	0.25	0.05	0.04	0.06	0.06	0.07	0.06	0.07	0.02
p8	Male	50	12/14/2023	Ide-cel	I	1.5	0.03	0	0.05		0.11	0.25	0.99	1.51	2.42
p9	Male	56	1/24/2024	Cilta-cel	I	2.25	0.15	0.18	0.26	0.3	0.32	0.17	0.28	0.23	0.14
p10	Female	60	1/24/2024	Cilta-cel	I	2.99	0.15	0.15	0.18	0.28	0.31	0.38	0.29	0.36	0.26
p11	Female	56	2/26/2024	Cilta-cel	II	0.99	0.25	0.2	0.25	0.26	0.27	0.29	0.25	0.19	0.15
p12	Male	55	3/13/2024	Cilta-cel	I	2.3	0.04	0.08	0.08	0.19	0.03	0.06	0.51	0.51	0.73
p13	Male	57	3/29/2024	Cilta-cel	Unknown	2.15	0.28	0.16	0.26	0.44	0.46	0.45	0.38	0.57	0.59
p14	Female	44	10/16/2024	Cilta-cel	III	1.6	0.01	0.01	0.01		0.15	0.33			
p15	Male	42	3/3/2025	Cilta-cel	I	0.26	0.06	0.04	0.09	0.21	0.47	0.58	0.62	0.69	2.15
p16	Male	65	6/10/2024	Cilta-cel	I	0.57	0.04	0.02	0.01	0.08	0.03	0.06	0.05	0.07	1.09
p17	Male	67	3/4/2025	Cilta-cel	I	0.5	0.04	0.03	0.02	0.09	0.02	0.02	0.02		0.34
p18	Male	65	8/28/2023	Cilta-cel	II	0.28	0.02	0.03	0.05	0.08	0.02	0.08	0.06	0.02	0.56
p19	Female	58	8/19/2024	Cilta-cel	I	0.01									
p20	Male	66	2/3/2025	Ide-cel	Unknown	0.18									
p21	Female	71	3/11/2025	Cilta-cel	Unknown	1.22		0.02	0.09	0.19	0.25	0.32	0.18	0.06	0.11

ALC_d9	ALC_d10	ALC_d11	ALC_d12	ALC_d13	ALC_d14	ALC_d15	ALCmax	%BCMA of T cells at ALCmax	% CD4 BCMA of T cells at ALCmax	% CD8 BCNA of T cells at ALCmax	CRS	CRS grade	CRS date	ICANS	ICANS grade	Delayed neurotoxicity
	0.34	0.84	3.53	4.27	2.83	1.62	4.27	54	35.5776	39.6494	Yes	Grade I	6/20/2023	No	NA	No
0.39	1.42	5.59	5.13	3.37	2.75	1.78	5.59	60	43.6433	12.2112	Yes	Grade I	7/24/2023	No	NA	No
		0.58	4.31	13.72	13.11	8.62	13.72	45.7	2.4684	0.9516	Yes	Grade II	9/19/2023	No	NA	No
0.91	1.43	1.69	1.31	0.82	0.59	0.84	1.69	11.7	0.645	0.5166	Yes	Grade II	9/18/2023	No	NA	No
0.22	0.15	0.35	0.58	1.25	1.22	0.65	1.25	31.3	14.5017	9.9588	Yes	Grade I	9/20/2023	No	NA	No
0.37	0.3	0.83	2.02	2.16	1.48	0.97	2.16	56.8	11.1154	34.4114	Yes	Grade I	9/29/2023	No	NA	No
0.1	0.22	0.4	0.42	0.57	0.63	0.29	0.63	25.1	4.3524	9.88	Yes	Grade II	11/10/2023	No	NA	No
1.41	1.26	0.95	0.71	0.68	0.8	0.7	2.42	6.6	1.092	2.6159	Yes	Grade I	12/14/2023	No	NA	No
0.31	1.27	4.51	3.76	2.48			4.51	24.7	4.212	21.7	Yes	Grade II	1/31/2024	No	NA	No
0.43	0.74	2.11	2.41	1.78			2.41	7.8	2.1667	5.029	No	NA		No	NA	No
1.33	10.04	25.98	23.03	14.09	6.12		25.98	74.3	30.7997	23.6145	Yes	Grade II	3/5/2024	No	NA	No
0.76					0.84		0.84	8.9	0.8575	7.116	Yes	Grade I	3/14/2024	No	NA	No
0.33	1.81	4.93	3.99	2.21	1.22	0.87	4.93	53.6	9.6141	35.9307	Yes	Grade III	4/5/2024	No	NA	No
0.57	0.47	1.19	1.33	1.48	1.35		1.48	56.6	12.2958	42.0644	Yes	Grade I	10/17/2024	No	NA	No
5.17	5.94					1.1	5.94	72.9	18.0256	52.371	No	NA		NA	NA	No
4.77	7.6	7.19	3.28	1.62	1.09		7.6	74.7	41.5548	32.6784	Yes	Grade I	6/14/2024	No	NA	Yes
4.5	11.13	10.41	5.37	3.39		2.27	11.13	86.5	57.9026	26.2235	Yes	Grade I	3/11/2025	No	NA	Yes
3.21	9.55	11.13	5.27	3.73	2.31	1.7	11.13	84.6	83.1548	3.34	Yes	Grade III	8/31/2023	Yes	Grade II	Yes
0.14	1.4	2.81	4.05	4.85	4.14	3.83	4.85	84.7	11.6178	80.1855	Yes	Grade I	8/23/2024	Yes	Grade III	Yes
0.05	0.05	0.16	0.08	0.03	0.02		0.16	66.5	64.8636	3.358	Yes	Grade II	2/4/2025	Yes	Grade II	No
0.11	1.66	3.46	9.1	7.03	3.3	2.05	9.1	64.3	43.416	18.9164	Yes	Grade II	3/18/2025	Yes	Grade I	No